

Spin-phonon coupling in orthorhombic $RMnO_3$ ($R=Pr, Nd, Sm, Eu, Gd, Tb, Dy, Ho, Y$): A Raman study

J. Laverdière and S. Jandl

Regroupement Québécois sur les Matériaux de Pointe, Département de Physique, Université de Sherbrooke, Sherbrooke, Canada J1 K 2R1

A. A. Mukhin and V. Yu. Ivanov

General Physics Institute, Russian Academy of Sciences, 119991 Moscow, Russia

V. G. Ivanov

Faculty of Physics, University of Sofia, 1164 Sofia, Bulgaria

M. N. Iliev

Texas Center for Superconductivity and Department of Physics, University of Houston, Texas 77204-5002, USA

(Received 3 January 2006; revised manuscript received 22 March 2006; published 6 June 2006)

The temperature-dependent Raman spectra of orthorhombic $RMnO_3$ ($R=Pr, Nd, Sm, Eu, Gd, Tb, Dy, Ho, Y$) were studied in the 5–300 K temperature range. It was established that while the materials with large R^{3+} ionic radius r_R and A -type antiferromagnetic order ($R=Pr, Nd, Sm$) exhibit significant phonon softening and other anomalies with decreasing temperature near and below T_N , the effect of magnetic ordering is much weaker or negligible in compounds with $R=Eu, Gd, Tb, Dy, Ho,$ and Y , characterized by small r_R and incommensurate magnetic structure. The results are discussed accounting for the variations with r_R of the type of magnetic ordering and related spin-phonon interaction.

DOI: [10.1103/PhysRevB.73.214301](https://doi.org/10.1103/PhysRevB.73.214301)

PACS number(s): 78.30.-j, 63.20.Dj, 75.47.Lx

I. INTRODUCTION

The rediscovery of colossal magnetoresistance in mixed valence perovskitelike manganites $R_{1-x}A_xMnO_3$ (R =rare earth or Y ; A =Sr, Ca, Ba, Pb)^{1–4} has attracted significant interest in the properties of the $RMnO_3$ parent compounds. It was recently demonstrated that the magnetic and orbital structures in these materials depend strongly on the ionic radius r_R of the rare earth ion.^{5,6} In particular, it was shown that the orbital ordering temperature T_{OO} monotonically increases with decreasing r_R , while the magnetic ordering temperature T_M decreases. Moreover, with decreasing r_R the low temperature antiferromagnetic (AFM) ordering changes from A -type AFM to E -type AFM (Ref. 6) through an incommensurate (IC) structure. The effect of r_R on the crystal structure is most clearly pronounced in the decrease of the Mn-O-Mn bond angle from 155° for $LaMnO_3$ ($r_{La}=1.032$ Å) to 144° for $HoMnO_3$ ($r_{Ho}=0.901$ Å). It is plausible to expect that the changes with r_R of the lattice distortions and magnetic structure will be reflected in changes of the phonon parameters and their variations near magnetic ordering temperature. Indeed, it has been established in the case of $LaMnO_3$ (Refs. 7–9) and $NdMnO_3$ (Ref. 10) that the magnetic ordering below T_N results in softening of a Raman active mode near 610 cm^{-1} , involving mainly in-plane stretching oxygen vibrations. This softening has been discussed by Granado *et al.*⁸ in terms of spin-phonon coupling caused by phonon modulation of the superexchange integral. The increase of orbital coherence length upon cooling and polaronic interaction of the e_g orbital electrons with phonons has also been invoked as a source of softening in $LaMnO_3$.^{11,12} The verification of theoretical models requires a more systematic study

of magnetic-ordering effects on the phonons in the $RMnO_3$ series, particularly through the change from A -type to E -type AF order. As a first step in this direction, we report and discuss results of a comparative study of temperature-dependent polarized Raman spectra of $PrMnO_3$, $NdMnO_3$, $SmMnO_3$, $EuMnO_3$, $GdMnO_3$, $TbMnO_3$, $DyMnO_3$, $HoMnO_3$, and $YMnO_3$.

II. SAMPLES AND EXPERIMENTAL

$PrMnO_3$, $NdMnO_3$, and $SmMnO_3$, single crystals were grown by the floating zone method described in Ref. 13. Single crystals of $DyMnO_3$ of average sizes $1 \times 1 \times 2\text{ mm}^3$ were prepared following a procedure to be described elsewhere.¹⁴ Orthorhombic $YMnO_3$, $HoMnO_3$ samples were prepared under pressure as described in Ref. 15. For samples with $R=Eu, Gd,$ and Tb , stoichiometric powders were heated at 1130 – 1160 °C under O_2 atmosphere for 24 h. The last five samples were polycrystalline from which selected microcrystals were larger than the laser spot. It was possible to select microcrystals with crystallographic orientations such that the spectra in parallel and crossed scattering configurations were dominated by A_g or B_{2g} contributions, respectively. For exact separation of the A_g and B_{2g} spectra the SPECTRA SUBTRACT program of the GRAMS AI software package was used.

The Raman spectra were measured in backscattering configuration using a Labram-800 Raman microscope spectrometer (spectral resolution 0.5 cm^{-1}) equipped with a liquid-nitrogen-cooled CCD detector and a micro-Helium Janis cryostat. The ($\lambda_{exc}=632.8\text{ nm}$) laser, focused on the sample through $10\times$ or $50\times$ objectives, was kept under extremely

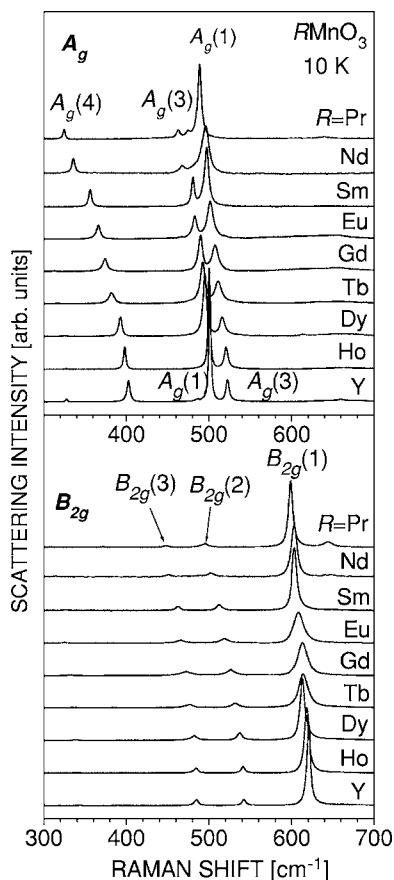


FIG. 1. Polarized Raman spectra of $RMnO_3$ ($R = \text{Pr, Nd, Sm, Eu, Gd, Tb, Dy, Ho, Y}$) as obtained at 10 K with $xx(A_g)$ and $xz(B_{2g})$ scattering configurations.

low irradiance (0.02 to 0.3 $\text{mW}/\mu\text{m}^2$ to avoid local heating).

III. EXPERIMENTAL RESULTS

Figure 1 shows the Raman spectra of $RMnO_3$ as obtained at 10 K in $xx(A_g)$ and $xz(B_{2g})$ scattering configurations. The Raman line notations are associated with the type of atomic motions of the corresponding phonon modes expected for the $Pnma$ structure. $A_g(1)$ and $B_{2g}(1)$ denote, respectively, anti-stretching and stretching vibrations of oxygen atoms in the xz planes, $A_g(3)$ and $B_{2g}(3)$ correspond to bendings of MnO_6 octahedra, $A_g(4)$ denotes MnO_6 rotations, and “ $B_{2g}(2)$ scissor-like” oxygen rotations.^{16,17} The shape of $A_g(1)$, $A_g(3)$, $A_g(4)$, and $B_{2g}(1)$ modes is shown in Fig. 2. With decreasing r_R most Raman lines shift towards higher frequencies. At the same time there is a transfer of intensity between the two high frequency A_g lines near 500 cm^{-1} . The latter phenomenon is observed in the whole temperature range and has been explained by the coupling of the $A_g(1)$ and $A_g(3)$ modes, which is weak for the end members of the $RMnO_3$ series, but particularly strong for $R = \text{Eu, Gd, Tb}$.¹⁷ For larger r_R ($R = \text{La, Pr, Nd}$) the lower line corresponds to bending [$A_g(3)$] vibrations. With decreasing r_R the line hardens and approaches the higher one [$A_g(1)$], which exhibits much weaker dependence on r_R . Due to the strong mode mixing,

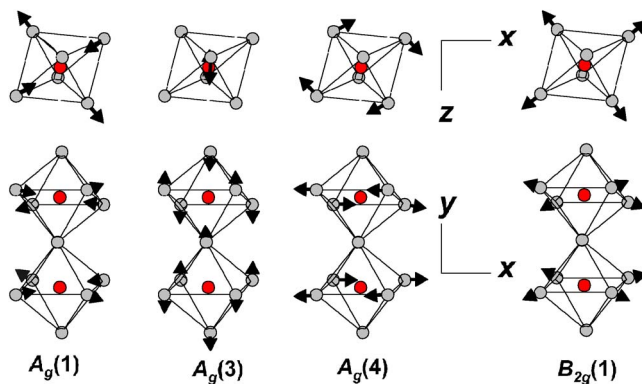


FIG. 2. (Color online) Main atomic motions of $A_g(1)$, $A_g(3)$, $A_g(4)$, and $B_{2g}(1)$ modes.

the two lines cannot any longer be denoted as $A_g(1)$ or $A_g(3)$ for intermediate r_R . With further decrease of r_R ($R = \text{Ho, Y}$) the modes become less coupled. At this end of the $RMnO_3$ series, however, the lower line represents the anti-stretching $A_g(1)$ mode.

$B_{2g}(1)$, $A_g(1)$, and $A_g(3)$ [or mixed $A_g(1)/A_g(3)$] modes frequencies are shown as a function of temperature in Fig. 3. The dashed line corresponds to the fit of experimental points above T_N with the function

$$\omega(T) = \omega_0 - C \left[1 + \frac{2}{e^{\omega_0/kT} - 1} \right], \quad (1)$$

where ω_0 and C are adjustable parameters. $\omega(T)$ describes expected temperature dependence of a phonon mode frequency due to anharmonic phonon-phonon scattering.¹⁸

With decreasing temperature the $B_{2g}(1)$ modes of PrMnO_3 , NdMnO_3 and SmMnO_3 soften by 1.1–1.2%, a value comparable to that reported for LaMnO_3 .⁷ Although it starts above T_N , the softening is most strongly pronounced below T_N . The $B_{2g}(1)$ modes of the other $RMnO_3$ samples do not soften at all except for DyMnO_3 which shows a much weaker softening ($\sim 0.3\%$) with no pronounced anomaly near T_N . The variations with R of the temperature dependence for the remaining Raman modes are similar except that, if observed, the softening is by a factor 2 to 5 weaker as compared to the $B_{2g}(1)$'s. This is illustrated in the right panels of Fig. 3 for the $A_g(1)$ and $A_g(3)$ [or mixed $A_g(1)/A_g(3)$] modes. The $RMnO_3$ compounds with large r_R exhibit another magnetic-order-related anomaly, namely, significant increase of the $B_{2g}(1)$ Raman line intensities below T_N (Fig. 4). No anomaly near T_N has been observed in the temperature dependence of the Raman linewidths.

IV. DISCUSSION

The orthorhombic $RMnO_3$ compounds with large r_R (from La to Sm) are characterized by A-type antiferromagnetic (AFM) structure.^{5,20–26} In this structure the Mn^{3+} moments are ferromagnetically (FM) ordered in the xz (ac) planes and antiferromagnetically coupled along the y (b) direction (in $Pnma$ notations). The Néel temperature T_N decreases from

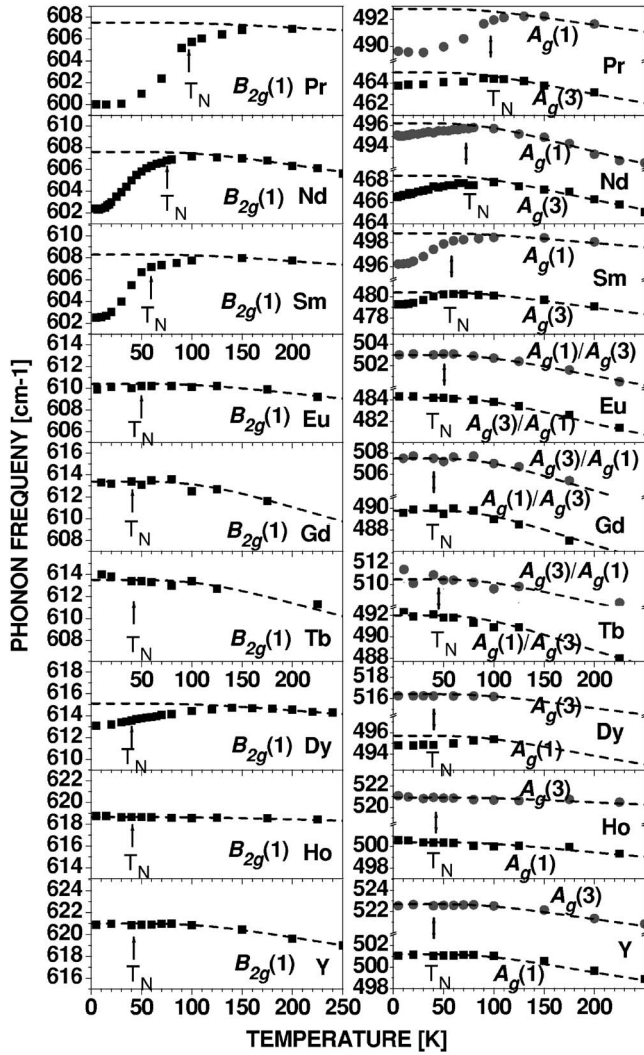


FIG. 3. Frequency variations with T 's of $B_{2g}(1)$ modes (left panels) and $A_g(1)$, $A_g(3)$, and mixed $A_g(1)/A_g(3)$ modes (right panels). Dashed lines correspond to Eq. (1).

97 K for PrMnO_3 to 76 K for NdMnO_3 and 60 K for SmMnO_3 .^{21–26} With increasing structural distortions, the magnetic structure of $R\text{MnO}_3$ compounds with small r_R (from Eu to Ho) changes to an incommensurate (IC) sinusoidal AFM structure characterized by a propagation vector $\mathbf{k}=(k_x, 0, 0)$.^{5,6,27,28} The origin of such frustrated structures below T_N has been associated with the weakening of the FM interaction between the nearest-neighbor (NN) e_g spins (allowing dominant AFM interaction between the NN t_{2g} spins) and the anisotropic super-exchange (SE) interaction between next-nearest-neighbor (NNN) Mn^{3+} moments.⁵ For $R=\text{Eu}$ and Gd, k_x decreases from $T_N=51$ and 40 K (Refs. 5 and 6) and A -type AFM and canted AFM structure¹⁹ develop at lower temperatures (46 and 26 K, respectively). In TbMnO_3 (DyMnO_3) the k_x component of \mathbf{k} varies from 0.295 (0.39) at 40 K to 0.28 (0.46) at 30 K (18 K) and remains locked at lower temperatures.⁵ Similarly, the k_x value for YMnO_3 increases from 0.420 at $T_N=42\text{K}$ and locks at 0.435 below 28 K.²⁸ For HoMnO_3 ($T_N=41\text{K}$), the k_x component increases from 0.40 and locks below 29 K at $k_x=0.5$, which

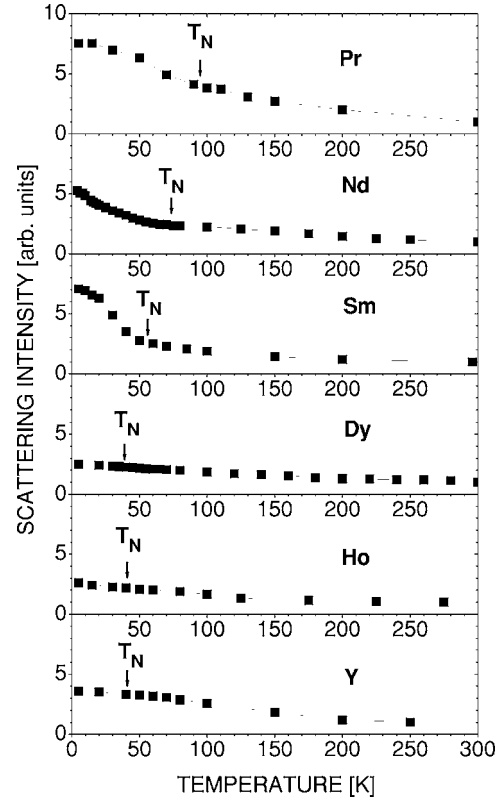


FIG. 4. Intensity variation with T of the $B_{2g}(1)$ stretching mode.

corresponds to the E -type AFM structure.²⁷ It is obvious from our experimental results that while the magnetic-order-induced phonon softening is strong in $R\text{MnO}_3$ with A -type AFM structure, it is either very weak or absent in the materials showing incommensurate or E -type AFM structure.

According to the mechanism proposed by Granado *et al.*⁸ the effect of phonon renormalization below T_N is proportional to the spin-spin correlation function $\langle \mathbf{S}_i \cdot \mathbf{S}_j \rangle$ for the nearest-neighbor spins localized at the i th and j th Mn^{3+} sites. In the case of LaMnO_3 where A -type ordering takes place the i th spin can be represented as

$$\mathbf{S}_i = \frac{\mathbf{M}}{4\mu_B} + \Delta\mathbf{S}_i,$$

where \mathbf{M} is the average sublattice magnetization per Mn^{3+} and $\Delta\mathbf{S}_i$ is the spin fluctuation due to quantum and thermal effects. In the work of Granado *et al.*⁸ the molecular-field approximation has been employed, which means that $\Delta\mathbf{S}_i$ is neglected and the phonon renormalization scales as \mathbf{M}^2 . This approximation explains fairly well the temperature behavior of the $B_{2g}(1)$ below T_N . However, as evident from the data for LaMnO_3 (Ref. 8) and as follows from our data for PrMnO_3 , NdMnO_3 , and SmMnO_3 , the onset of phonon renormalization is located at temperatures well above T_N . This fact has been observed but not discussed by Granado *et al.*⁸ The renormalization of phonon frequencies above T_N can be explained by in-plane ferromagnetic correlations $\langle \Delta\mathbf{S}_i \cdot \Delta\mathbf{S}_j \rangle$ which exist even in the paramagnetic phase.

In order to analyze the cases of incommensurate and E -type ordering, an extension to the above model is necessary. Those orderings result from competition between the ferromagnetic NN and antiferromagnetic NNN interactions. As proposed by Kimura *et al.*⁵ the incommensurate phases are described by a three-parameter frustrated exchange Hamiltonian

$$H = \frac{1}{2} \sum_{i,r} J(\mathbf{r}) \mathbf{S}_i \cdot \mathbf{S}_{i+r}, \quad (2)$$

where $J(\mathbf{r})=J_1 < 0$ is a ferromagnetic exchange between NN spins ($\mathbf{r}=\pm 0.5\mathbf{x}\pm 0.5\mathbf{z}$), $J(\mathbf{r})=J_2 > 0$ is an antiferromagnetic exchange between NNN spins along x ($\mathbf{r}=\pm\mathbf{x}$), and $J(\mathbf{r})=J_3 < 0$ is a very weak ferromagnetic coupling between NNN for $\mathbf{r}=\pm\mathbf{z}$. Thus, following Ref. 8 we obtain for the phonon renormalization

$$\Delta\omega = \frac{1}{2m\omega} \sum_r \frac{\partial^2 J(\mathbf{r})}{\partial u^2} \langle \mathbf{S}_i \cdot \mathbf{S}_{i+r} \rangle, \quad (3)$$

where ω represents the mode frequency, m the oxygen mass, u the oxygen displacement.

For an incommensurate phase with $\mathbf{k}=(k_x, 0, 0)$ the spin-spin correlation function is

$$\langle \mathbf{S}_i \cdot \mathbf{S}_{i+r} \rangle = K(T) \cos(2\pi\mathbf{k} \cdot \mathbf{r}),$$

where $K(T)$ is a temperature-dependent prefactor. Thus, restricting summation up to NNN Mn ions, we get

$$\Delta\omega = \frac{K(T)}{m\omega} [2D_1 \cos(\pi k_x) + D_2 \cos(2\pi k_x) + D_3], \quad (4)$$

where $D_j = \partial^2 J_j / \partial u^2$ ($j=1, 2, 3$).

Our further analysis is based on Eq. (4). For A -type materials ($R=\text{La, Nd, Pr, Sm}$) $\mathbf{k}=0$, $K(T) \propto M_{\text{sublatt}}^2$, and we obtain a nonzero phonon softening below T_N , provided $2D_1 + D_2 + D_3 < 0$. The expression of Granado *et al.*⁸ for the softening of B_{2g} mode

$$\Delta\omega \approx \frac{2}{m\omega} \frac{\partial^2 J_1}{\partial u^2} \left(\frac{M_{\text{sublatt}}(T)}{4\mu_B} \right)^2 \quad (5)$$

corresponds to the approximation $|D_1| \gg |D_2 + D_3|$.

For an E -type ordering ($R=\text{Ho}$) $k_x=0.5$ and we obtain $\Delta\omega \propto K(T)(D_3 - D_2)$. As evident, in this case the NN contributions exactly cancel each other since each Mn ion is surrounded by two spin-up and two spin-down ions. The finding that no phonon softening is observed in the E -phase means that the second derivatives D_2 and D_3 of the NNN exchange integrals are equal between themselves, at least to the accuracy limit of the Raman-frequency measurements. This fact can be interpreted in the frame of a more general symmetry consideration. The NNN exchange integral $J(\mathbf{r})$ can be represented as

$$J(\mathbf{r}) = J_s(\mathbf{r}) + J_d(\mathbf{r}), \quad (6)$$

where the s -type function $J_s(\mathbf{r})$, transformed as $x^2 + z^2$, is characteristic for an idealized tetragonal structure, while the $x^2 - z^2$ contribution from $J_d(\mathbf{r})$ arises due to the orthorhombic distortion of the lattice. It is $J_d(\mathbf{r})$ which is responsible for

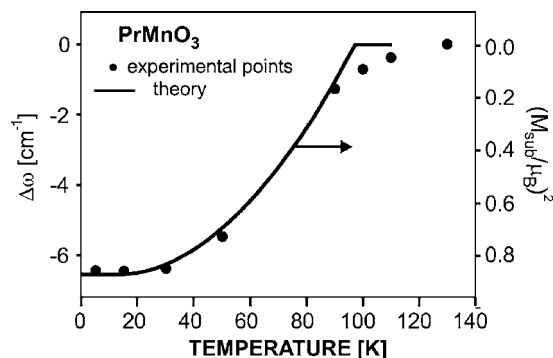


FIG. 5. Temperature shift of the PrMnO₃ $B_{2g}(1)$ stretching mode frequency. The line represents the square of M_{sublatt}/μ_B calculated in the mean field approximation.

the $J_2 - J_3$ asymmetry. Thus the equality between D_2 and D_3 implies that the Raman-active phonons in $R\text{MnO}_3$ modulate only the s -wave contribution to the exchange integral. This fact may have an important impact on understanding the spin and orbital ordering in the insulating manganites.

Bearing in mind that $D_2 \approx D_3$ we obtain for intermediate k_x values

$$\Delta\omega = \frac{K(T)}{m\omega} \{2D_1 \cos(\pi k_x) + D_2 [1 + \cos(2\pi k_x)]\}. \quad (7)$$

Hence, depending on the relative sign and magnitude of D_1 and D_2 in the case of incommensurate magnetic ordering one may have a null effect or phonon renormalization.

Equation (5) describes quite well the softening of the $B_{2g}(1)$ mode in PrMnO₃, NdMnO₃, and SmMnO₃ as illustrated in Fig. 5 for the case of PrMnO₃. Given that, in a good approximation, the B_{2g} frequencies are nearly independent of R and with the known maximum Mn³⁺ μ values for PrMnO₃ ($\mu \approx 3.5$), NdMnO₃ [$\mu=3.22$ (Ref. 23)], and SmMnO₃ [$\mu=3.5$ (Ref. 26)], the $\partial^2 J_1 / \partial u^2$ values of ≈ 15.5 mRy/Å², ≈ 13.5 mRy/Å², and ≈ 12.9 mRy/Å² for PrMnO₃, NdMnO₃ and SmMnO₃, respectively, were obtained using Eq. (5). For LaMnO₃ [$\mu=3.65$ (Ref. 29)] a $\partial^2 J_{xz} / \partial u^2$ value of ≈ 16 mRy/Å² has been reported.⁸

Although our model shows that a phonon renormalization, due to spin-phonon coupling is possible, such is undetectable in the incommensurate antiferromagnetic phase of EuMnO₃, GdMnO₃, TbMnO₃, HoMnO₃, and YMnO₃. The clear absence of phonon softening in EuMnO₃ and GdMnO₃, however, challenges the association of magnetic structure below 46 and 26 K, respectively, with A -type AFM ordering.⁵ The weak softening observed for B_{2g} and A_g stretching modes in DyMnO₃ starts well above T_N and may be related to a small expansion in the Mn-O distances rather than to direct spin-phonon coupling. A careful study of the Mn-O distance temperature variations may help elucidate its origin.

The increase in intensity of the phonon modes, which exhibit strong softenings in A -type AFM compounds (Fig. 4), obviously correlates with FM ordering in the xz layers. At present there is no plausible explanation of this effect.

V. CONCLUSION

In summary, we have studied the temperature-dependent Raman spectra of orthorhombic $RMnO_3$ ($R = \text{Pr, Nd, Sm, Eu, Gd, Tb, Dy, Ho, Y}$) and have unambiguously established a correlation between FM ordering in the xz layers and phonon softening and intensity increase below T_N . The variations with temperature of the phonon line positions have allowed us to estimate $\partial^2 J_1 / \partial u^2$ contribution to B_{2g} stretching mode concluding that the spin-phonon coupling remains nearly the same for all A -type AFM compounds. The spin-phonon coupling is negligible in $RMnO_3$ with small r_R and incommensurate AFM. For E -type AFM

order ($R = \text{Ho}$), absence of phonon anomaly indicates that the NNN exchange integrals are equal.

ACKNOWLEDGMENTS

We thank M. Gospodinov and Y.-Q. Wang for the $DyMnO_3$, $EuMnO_3$, $GdMnO_3$, and $TbMnO_3$ samples. This work was supported by the National Science and Engineering Research Council of Canada, the Fonds Québécois de la Recherche sur la Nature et les Technologies and the State of Texas through the Texas Center for Superconductivity. V. G. I. acknowledges partial support by the French-Bulgarian bilateral Project No. PAI-RILA 2/5 and Grant No. UFNI-65 of the University of Sofia.

-
- ¹R. M. Kusters, J. Singleton, D. A. Keen, R. McGreevy, and W. Hayes, *Physica B* **155**, 362 (1989).
- ²R. von Helmolt, J. Wecker, B. Holzapfel, L. Schultz, and K. Samwer, *Phys. Rev. Lett.* **71**, 2331 (1993).
- ³S. Jin, T. H. Tiefel, M. McCormack, R. A. Fastnacht, R. Ramesh, and L. H. Chen, *Science* **64**, 413 (1994).
- ⁴Y. Tokura, A. Urushibara, Y. Moritomo, T. Arima, A. Asamitsu, G. Kido, and N. Furukawa, *Science* **63**, 3931 (1994).
- ⁵T. Kimura, S. Ishihara, H. Shintani, T. Arima, K. T. Takahashi, K. Ishizaka, and Y. Tokura, *Phys. Rev. B* **68**, 060403(R) (2003).
- ⁶T. Goto, T. Kimura, G. Lawes, A. P. Ramirez, and Y. Tokura, *Phys. Rev. Lett.* **92**, 257201 (2004).
- ⁷E. Granado, N. O. Moreno, A. García, J. A. Sanjurjo, C. Rettori, I. Torriani, S. B. Oseroff, J. J. Neumeier, K. J. McClellan, S. W. Cheong, and Y. Tokura, *Phys. Rev. B* **58**, 11435 (1998).
- ⁸E. Granado, A. García, J. A. Sanjurjo, C. Rettori, I. Torriani, F. Prado, R. Sánchez, A. Caneiro, and S. B. Oseroff, *Phys. Rev. B* **60**, 11879 (1999).
- ⁹M. N. Iliev and M. V. Abrashev, *J. Raman Spectrosc.* **32**, 805 (2001).
- ¹⁰S. Jandl, S. N. Barilo, S. V. Shiryaev, A. A. Mukhin, V. Yu. Ivanov, and A. M. Balbashov, *J. Magn. Magn. Mater.* **264**, 36 (2003).
- ¹¹J. van den Brink, *Phys. Rev. Lett.* **87**, 217202 (2001).
- ¹²J. Bala, A. M. Oleś, and G. A. Sawatzky *Phys. Rev. B* **65**, 184414 (2002).
- ¹³A. M. Balbashov, S. G. Karabashev, Y. A. M. Mukovskii, and S. A. Zverkov, *J. Cryst. Growth* **167**, 365 (1996).
- ¹⁴M. M. Gospodinov (unpublished).
- ¹⁵M. N. Iliev, A. P. Litvinchuk, Y.-Q. Wang, Y. Y. Sun, and C. W. Chu, *Physica B* **358**, 138 (2005).
- ¹⁶M. N. Iliev, M. V. Abrashev, H. G. Lee, V. N. Popov, Y. Y. Sun, C. Thomsen, R. L. Meng, and C. W. Chu, *Phys. Rev. B* **57**, 2872 (1998).
- ¹⁷M. N. Iliev, M. V. Abrashev, J. Laverdière, S. Jandl, M. M. Gospodinov, Y.-Q. Wang, and Y. Y. Sun, *Phys. Rev. B* **73**, 064302 (2006).
- ¹⁸M. Balkanski, R. F. Wallis, and E. Haro, *Phys. Rev. B* **28**, 1928 (1983).
- ¹⁹J. Hemberger, S. Lobina, H.-A. Krug von Nidda, N. Tristan, V. Yu. Ivanov, A. A. Mukhin, A. M. Balbashov, and A. Loidl, *Phys. Rev. B* **70**, 024414 (2004).
- ²⁰R. Pauthenet and C. Veyret, *J. Phys. (France)* **31**, 65 (1970).
- ²¹J. Hemberger, M. Brando, R. Wehn, V. Yu. Ivanov, A. A. Mukhin, A. M. Balbashov, and A. Loidl, *Phys. Rev. B* **69**, 064418 (2004).
- ²²A. A. Mukhin, V. Yu. Ivanov, V. D. Travkin, and A. M. Balbashov, *J. Magn. Magn. Mater.* **226-230**, 1139 (2001).
- ²³A. Munoz, J. A. Alonso, M. J. Martínez-Lope, J. L. García-Munoz, and M. T. Fernández-Díaz, *J. Phys.: Condens. Matter* **12**, 1361 (2000).
- ²⁴A. A. Mukhin, V. Yu. Ivanov, V. D. Travkin, A. S. Prokhorov, A. M. Balbashov, J. Hemberger, and A. Loidl, *J. Magn. Magn. Mater.* **272-276**, 96 (2004).
- ²⁵S. Y. Wu, C. M. Kuo, H. Y. Wang, W.-H. Li, K. C. Lee, J. W. Lynn, and R. S. Liu, *J. Appl. Phys.* **87**, 5822 (2000).
- ²⁶V. Yu. Ivanov, A. A. Mukhin, A. S. Prokhorov, and A. M. Balbashov, *Phys. Status Solidi B* **236**, 445 (2003).
- ²⁷A. Munoz, M. T. Casáis, J. A. Alonso, M. J. Martínez-Lope, J. L. Martínez, and M. T. Fernández-Díaz, *Inorg. Chem.* **40**, 1020 (2001).
- ²⁸A. Munoz, J. A. Alonso, M. T. Casais, M. J. Martínez-Lope, J. L. Martínez, and M. T. Fernández-Díaz, *J. Phys.: Condens. Matter* **14**, 3285 (2002).
- ²⁹Q. Huang, A. Santoro, J. W. Lynn, R. W. Erwin, J. A. Borchers, J. L. Peng, and R. L. Greene, *Phys. Rev. B* **55**, 14987 (1997).